

25th ABCM International Congress of Mechanical Engineering
October 20-25, 2019, Uberlândia, MG, Brazil

COB-2019-0258

A PARAMETRIC ANALYSIS OF THE NONLINEAR DYNAMICS OF A DUFFING OSCILLATOR

Luã Guedes Costa

Luciana Loureiro da Silva Monteiro

Centro Federal de Educação Celso Suckow da Fonseca – CEFET/RJ – Mechanical Engineering Graduate Program 229 Maracanã Av. – Rio de Janeiro – RJ – Brazil – 27271-110

lua.costa@aluno.cefet-rj.br, lucianals.monteiro@gmail.com

Marcelo Amorim Savi

Universidade Federal do Rio de Janeiro – COPPE – Department of Mechanical Engineering Center for Nonlinear Mechanics – MECANON – Rio de Janeiro – RJ – Brazil – 21.941.972

savi@mecanica.ufrj.br

Abstract. *This contribution deals with a parametric analysis of a Duffing oscillator. Nonlinear stiffness coefficients are investigated treating monostable and bistable systems. Besides, the external forcing is evaluated on system dynamics, mapping and quantifying different types of responses of the dynamical system. Numerical simulations are employed using fourth order Runge-Kutta method and Lyapunov exponents are used to define chaotic behavior. A statistical analysis is developed establishing the probability of each kind of response to occur. Results show a variety of complex behaviors associated with bistable systems.*

Keywords: *Nonlinear Dynamics, Duffing Oscillator, Chaos, Lyapunov Exponents, Energy Harvesting Systems.*

1. INTRODUCTION

The classical Duffing oscillator is used to describe a great variety of physical phenomena. Mechanical and electrical nonlinear systems are usually employed to represent this kind of oscillator, establishing experimental basis for different investigations. In general, Duffing-type oscillators may present periodic and chaotic responses and a vast literature is dedicated to exploit the main aspects of this kind of system, such as: Moon and Holmes (1979), Moon (1992), Tam and Holmes (2014) and Hikiyama and Kawagoshi (1996) exploring the dynamic aspects of a magnetoelastic beam; Gottwald *et al.* (1992) who developed an experimental apparatus that mimic Duffing-type systems; Fouda *et al.* (2016) who investigated chaotic behavior in electrical Duffing-type circuits; Zaher (2018) who developed a technique that utilizes chaotic responses of the Duffing oscillator for secure communications; and Ferrari *et al.* (2010), Erturk and Inman (2011), Cellular *et al.* (2018) and Paula *et al.* (2015) who investigated bistable piezomagnetoelastic energy harvesting structures. In order to successfully design a Duffing-type system, parametric analysis is essential. Due to the complex nonlinear dynamics of these systems, this analysis is always revisited in order to define new strategies. The definition and classification of different kinds of response is an essential task that need to be associated with appropriate tools. In this regard, chaotic behavior is an important response that can be desirable or undesirable depending on the application. Lyapunov exponents is usually an accepted tool to define chaos and the method proposed by Wolf *et al.* (1985) is a good alternative for this aim. This contribution develops a numerical investigation in order to map and quantify the different kinds of responses of a Duffing-type one degree of freedom oscillator. This analysis is useful for different design purposes especially the ones related to energy harvesting systems.

2. MATHEMATICAL BACKGROUND

The classical forced Duffing oscillator is mathematically described by the following dimensionless equation of motion,

$$\ddot{u} + \zeta \dot{u} + \alpha u + \beta u^3 = \gamma \sin(\Omega t) \quad (1)$$

where ζ is the damping coefficient, γ is the forcing amplitude, Ω is the forcing frequency, α and β are nonlinear dimensionless stiffness coefficients that define the restitution force, $F(u) = \alpha u + \beta u^3$. Acceleration, velocity and position are represented by \ddot{u} , \dot{u} and u , respectively, and t is the time.

The equilibrium points $(\bar{u}, \dot{\bar{u}})$ of the system occur when velocity and acceleration are zero, therefore 3 points are

identified:

$$(\bar{u}, \dot{\bar{u}}) = (0, 0), \quad (\bar{u}, \dot{\bar{u}}) = \left(\sqrt{\frac{-\alpha}{\beta}}, 0 \right), \quad (\bar{u}, \dot{\bar{u}}) = \left(-\sqrt{\frac{-\alpha}{\beta}}, 0 \right) \quad (2)$$

Stability analysis shows that if $\alpha \geq 0$, the system is monostable with one stable equilibrium point at $(\bar{u}, \dot{\bar{u}}) = (0, 0)$. However, if $\alpha < 0$ the system is bistable with one unstable at $(\bar{u}, \dot{\bar{u}}) = (0, 0)$ and two stable points at $(\bar{u}, \dot{\bar{u}}) = (\pm\sqrt{-\alpha/\beta}, 0)$. This analysis can be clarified from the potential energy function, presented in Equation 3, that presents a double-well potential for a bistable system and a single-well potential for a monostable system, (Savi, 2017).

$$H(u) = \int F(u)du = \frac{1}{2}\alpha u^2 + \frac{1}{4}\beta u^4 \quad (3)$$

In monostable cases, the system oscillates around the single stable equilibrium point. In bistable cases, the system can either oscillate around one stable equilibrium point visiting one well, or jump between the two wells, visiting the two stable equilibrium points. Figure 1 shows the curves for restitution force and the potential energy of the system. The bottom of the wells represent the stable equilibrium points of the system. Also, for bistable cases, this curves show the necessary energy for the system to jump from one equilibrium point to another.

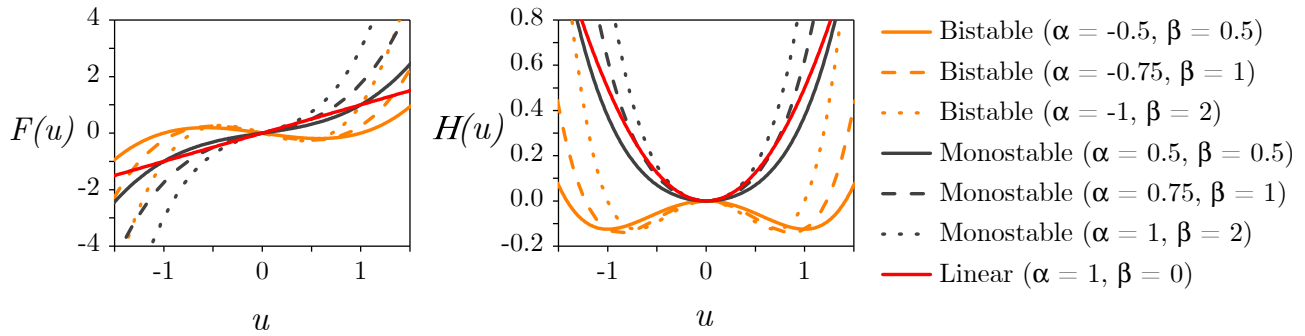


Figure 1: Restitution force and potential energy for different values of α and β .

3. NUMERICAL RESULTS AND DISCUSSION

Numerical simulations are carried out employing the fourth order Runge-Kutta method. Lyapunov exponents are estimated using the method proposed by Wolf *et al.* (1985). The parametric analysis is developed by building response maps that identify different kinds of response, classifying periodic and aperiodic regions. The procedure to build the maps uses the same initial conditions, u_0 and \dot{u}_0 , for all values of α and β , analyzing 1000 forcing periods, considering the last 250 as permanent regime. Table 1 shows the parameters employed in numerical simulations. Table 2 presents a response classification for the analysis. Note that different kinds of periodic motions are identified, together with chaotic responses. Escape points are related to responses different from the classified ones. The identification of each kind of response is based on Poincaré section recurrence analysis. Therefore, the steady-state response is evaluated in order to identify the system response. Lyapunov exponents are employing to assure chaotic-like responses.

Table 1: Duffing oscillator parameter ranges employed for the parametric analysis.

ζ	α	β	γ	Ω	u_0	\dot{u}_0
0.05	$-1 \rightarrow 1$	$0 \rightarrow 2$	$0.01 \rightarrow 1.5$	1	0	0

Figure 2 shows the response maps of the Duffing oscillator varying the stiffness coefficients considering different values of the forcing amplitude. It is noted that increasing the forcing amplitude, response areas are squeezed while new patterns emerge. Figure 2a and 2b shows that for very low forcing values the system tends to be periodic. The occurrence of chaotic regions in Figure 2c suggests that the system have enough energy to jump between equilibrium points for almost all values of β and negative α above and within the red region. Chaotic responses tend to diminish when γ increases, followed by a increase of period-2, period-3 and period-6+ responses for higher values of γ .

Table 2: Color legend for response types.

●	●	●	●	●	●	●	○
Period-1	Period-2	Period-3	Period-4	Period-5	Period-6+	Chaotic	Escape Points

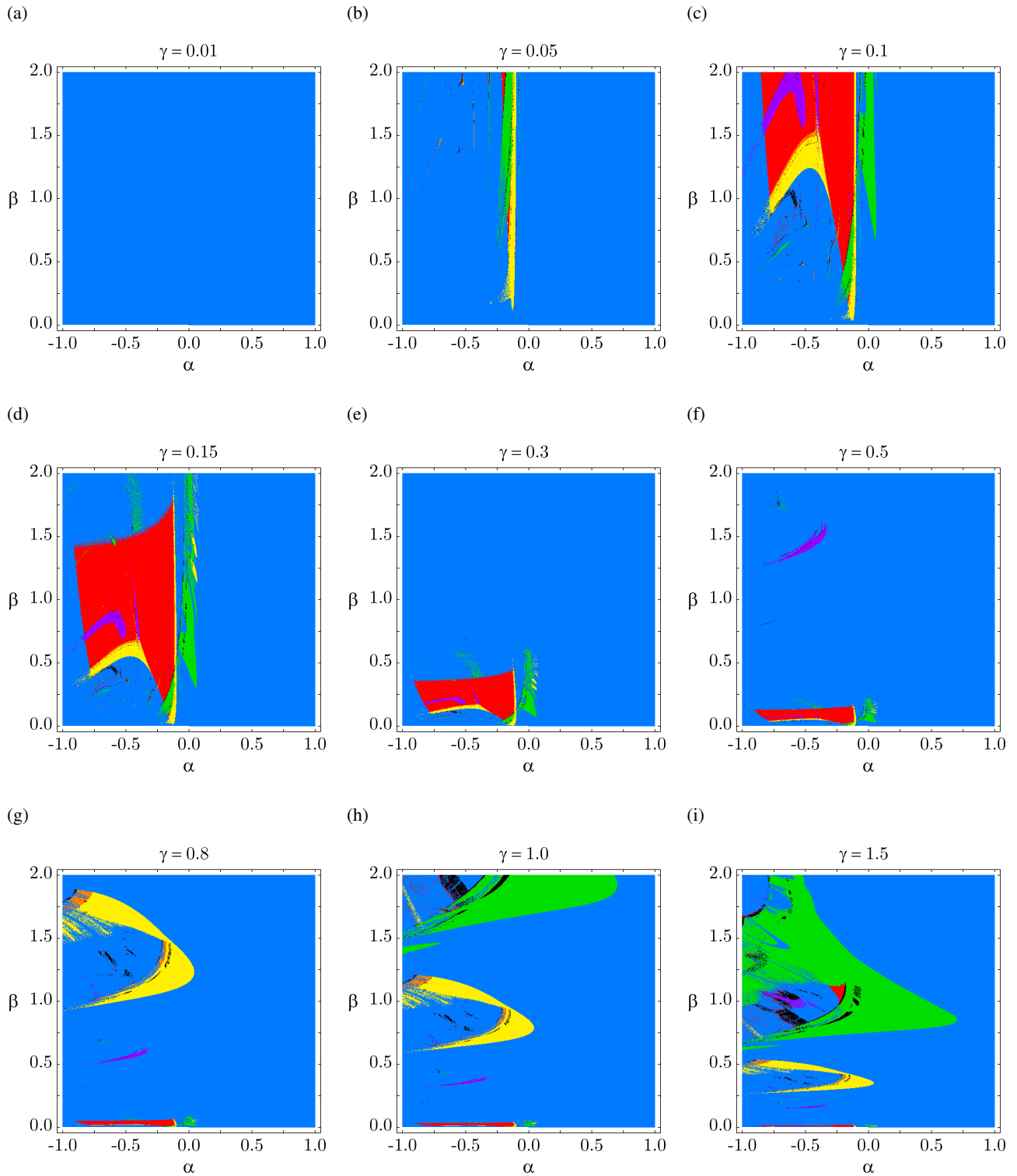


Figure 2: Response maps of the Duffing oscillator for different magnitudes of forcing amplitude. (a) $\gamma = 0.01$, (b) $\gamma = 0.05$, (c) $\gamma = 0.1$, (d) $\gamma = 0.15$, (e) $\gamma = 0.3$, (f) $\gamma = 0.5$, (g) $\gamma = 0.8$, (h) $\gamma = 1.0$ and (i) $\gamma = 1.5$.

Figures 3 and 4 quantify the amount of occurrence of each kind of response for a range of values of γ . Bistable and monostable cases, and the whole scope of the maps are considered. Colors in the graphs represent the same behavior described in Table 2, except escape points that are represented by gray color. For bistable systems, there is a peak presence of chaotic areas and a almost proportional decrease of period-1 responses on maps whose forcing amplitude is relatively low. For medium values of γ , the maps display a rapid increase of period-1 and the decay of chaotic responses. For high values, a small increase of period-2 regions is observed. Finally for very high forcing amplitudes, there is a rapid increase of period-3 regions almost proportional to a decrease in period-1 responses. For monostable systems, there is a predominance of period-1 regions for $\gamma < 1$, and the appearance of period-3 regions for $\gamma > 1$. Nevertheless, for all forcing values, the dominance of period-1 response regions is observed when considering the whole scope of the maps (bistable + monostable).

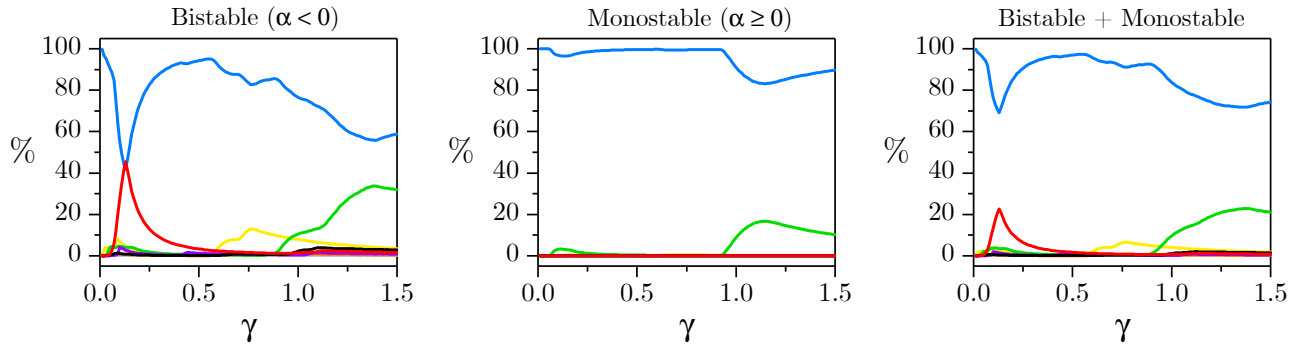


Figure 3: Occurrence of system responses for each stability condition and for the full scope of the maps.

In all cases, responses with periodicity above 3 tend to occupy small regions on the maps, being less prevalent. Figure 4 shows the occurrence of these regions. For the extension of γ values analyzed, high periodicity responses occur only in bistable systems, and have its peak when the forcing amplitude is relatively low ($\gamma < 0.5$) or very high ($\gamma > 1$).

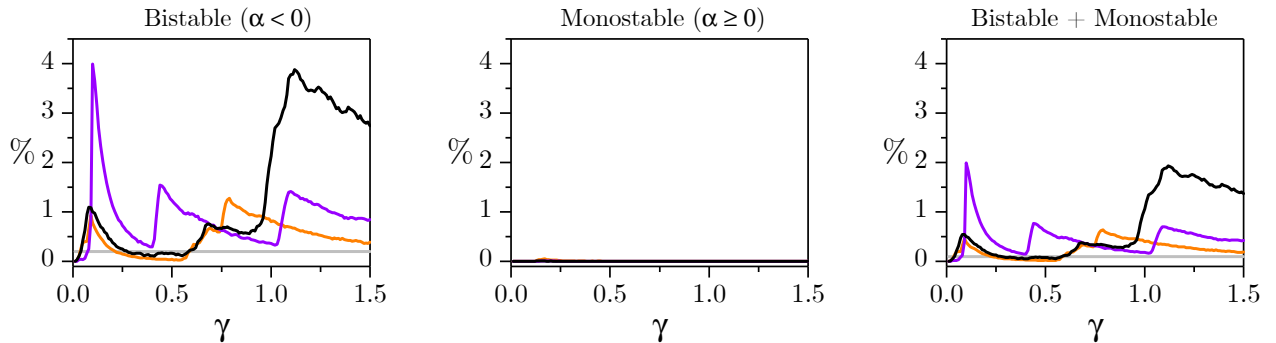


Figure 4: Occurrence of high periodicity system responses for each stability condition and for the full scope of the maps.

4. CONCLUSION

This paper presents an alternative approach to analyze Duffing-type systems. Classical numerical procedures as fourth order Runge-Kutta method and Lyapunov exponents are employed to build response maps that identify chaotic and periodic regions referring to the order of periodicity. These maps allow one to analyze monostable and bistable systems, identifying response patterns. It is clear that monostable system tends to be more stable while bistable systems tend to present more complex behaviors. In general, for lower forcing amplitudes, the system tends to behave more chaotically while for mid-high forcing amplitudes, period-2, period-3 responses tend to increase. However, for all cases, period-1 responses are dominant. This analysis shows that system response maps can be a useful tool to design and chose the optimal parameters of a Duffing-type system accordingly. Among the application where this strategy can be useful, it should be highlighted piezomagnetoelastic energy harvesting system.

5. ACKNOWLEDGEMENTS

The authors would like to acknowledge the support of the Brazilian Research Agencies CNPq, CAPES and FAPERJ. The support of the AFOSR is also acknowledged.

6. REFERENCES

- Cellular, A.C., da Silva Monteiro, L.L. and Savi, M.A., 2018. "Numerical investigation of nonlinear mechanical and constitutive effects on piezoelectric vibration-based energy harvesting". *Technisches Messen*, Vol. 85(9), pp. 565–579.
- Erturk, A. and Inman, D., 2011. "Broadband piezoelectric power generation on high-energy orbits of the bistable duffing oscillator with electromechanical coupling". *Journal of Sound and Vibration*, Vol. 330, No. 10, pp. 2339 – 2353.
- Ferrari, M., Ferrari, V., Guizzetti, M., Andò, B., Baglio, S. and Trigona, C., 2010. "Improved energy harvesting from wideband vibrations by nonlinear piezoelectric converters". *Sensors and Actuators A: Physical*, Vol. 162, No. 2, pp. 425 – 431.
- Fouda, J.A.E., Bodo, B., Djeufa, G.M. and Sabat, S.L., 2016. "Experimental chaos detection in the duffing oscillator". *Communications in Nonlinear Science and Numerical Simulation*, Vol. 33, pp. 259 – 269.
- Gottwald, J.A., Virgin, L.N. and Dowell, E.H., 1992. "Experimental mimicry of duffing's equation". *Journal of Sound and Vibration*, Vol. 158(3), pp. 447–467.
- Hikiyama, T. and Kawagoshi, T., 1996. "An experimental study on stabilization of unstable periodic motion in magneto-elastic chaos". *Physics Letters A*, Vol. 211, No. 1, pp. 29 – 36.
- Moon, F. and Holmes, P., 1979. "A magnetoelastic strange attractor". *Journal of Sound and Vibration*, Vol. 65, No. 2, pp. 275 – 296.
- Moon, F.C., 1992. *Chaotic and Fractal Dynamics*. John Wiley & Sons, Inc.
- Paula, A.S.D., Inman, D.J. and Savi, M.A., 2015. "Energy harvesting in a nonlinear piezomagnetoelastic beam subjected to random excitation". *Mechanical Systems and Signal Processing*, Vol. 54-55, pp. 405 – 416.
- Savi, M.A., 2017. *Dinâmica Não-Linear e Caos*. e-papers, Rio de Janeiro, 2nd edition.
- Tam, J.I. and Holmes, P., 2014. "Revisiting a magneto-elastic strange attractor". *Journal of Sound and Vibration*, Vol. 333, No. 6, pp. 1767 – 1780.
- Wolf, A., Swift, J.B., Swinney, H.L. and Vastano, J.A., 1985. "Determining lyapunov exponents from a time series". *Physica 16D*, pp. 285–317.
- Zaher, A.A., 2018. "Duffing oscillators for secure communication". *Computers and Electrical Engineering*, Vol. 71, pp. 77–92.

7. RESPONSIBILITY NOTICE

The authors are the only responsible for the printed material included in this paper.